https://doi.org/10.5194/egusphere-2026-4621
Preprint. Discussion started: 12 August 2026

Bank Pull or Bar Push: Who Leads the Dance of Meander Migration?

Gustavo W. Nagel, Stephen Darby, Julian Leyland, Eli D Lazarus

School of Geography and Environmental Sciences, University of Southampton,

Southampton, SO17 1BJ, UK

Laboratory example, city, postal code, country

Correspondence to: *Gustavo Willy Nagel* (angie@email.com)

Abstract. Despite significant advances in the study of meandering rivers, the precise mechanisms by which erosion and sedimentation interact to drive meander migration remain poorly understood. Two long-standing competing theories attempt to explain this interaction: one suggests that inner-bank sediment deposition precedes outer-bank erosion (bar push), while the other posits that outer-bank erosion initiates inner-bank sedimentation (bank pull). To date, empirical research addressing which of these mechanisms dominates in real-world environments has predominantly focused on a small number of bends and at limited temporal scales. In this paper, we identify analyse the occurrence of bank pull versus bar push across 4,923 river bends worldwide. We estimated outer-bank erosion and inner-bank sedimentation rates using a 38-year time series of Landsat data, from which classifications of bank pull and bar push were derived through Dynamic Cross-Correlation analysis. Of the 4,923 bends analyzed, 20% were classified as bank pull dominated, 16% as bar push dominated, whilst the remaining 63% showed no clear migration signal. We also identified river characteristics that control the relative frequency of push versus pull migrating bends. Our findings indicate that vegetated bends, with higher soil compactness surrounded by sandy substrates and situated in rivers with slower flow velocities, are more likely to exhibit bend migration via bar push, where sediment deposition along the inner bank plays a dominant role. In contrast, less densely vegetated rivers with higher flow velocities and lower soil compactness show a higher occurrence of bends migrating via bank pull. This means that most bar-push migrating bends are located in densely vegetated tropical environments, with bar pull tending to dominate in other regions. This study represents the first quasi-global empirical framework capable of distinguishing the temporal sequencing of erosion and sedimentation across thousands of river bends using long-term satellite observations, providing valuable insights that could be used to improve river dynamics modelling and inform more effective river management strategies.

1. Introduction

Meandering rivers sculpt intricate landscapes, characterized by sinuous channels and oxbow lakes, creating favourable conditions for communities and biodiversity to thrive (Gualtieri et al., 2020; Luize et al., 2018; Sabo et al., 2005; Zinger et al., 2013). These rivers form under specific topographic and hydrological conditions, requiring for example an adequate sediment supply to form point bars, sustained perturbations (e.g., an initial curvature to initiate the meandering process), and sufficient bank strength to prevent braiding (Braudrick et al., 2009; Nagabhushanaiah, 1967; van Dijk et al., 2012). They migrate laterally across their floodplains as a result of two processes: erosion on the outer bank and sedimentation on the inner bank of the bend. The faster flow velocities and higher shear stresses along the outer bank favour bank erosion there (Dietrich et al., 1979b). In contrast, slower velocities and reduced shear stresses at the inner bank create more favourable conditions for sediment deposition and point bar growth (Braudrick et al., 2009; Dietrich et al., 1979; Hickin & Nanson, 1975; Schumm & Khan, 1971; Schwendel et al., 2015).

Many modelled descriptions of river migration assume that outer bank erosion is directly influenced by the flow intensity, with inner bank sedimentation passively following to maintain a river width that is constant through time (Ikeda et al., 1981). This assumption is supported by long-term observations showing that, on average, river width remains relatively stable over extended periods (Lopez Dubon & Lanzoni, 2019). Recent studies, however, have documented how river width may fluctuate over time in response to environmental conditions, including variations in vegetation, hydroclimate, sediment supply, and the physical properties of the channel bed and banks (Akinola et al., 2019; Anderson et al., 2004; Chin, 2006; Francalanci et al., 2020). Moreover, processes of bank erosion and sedimentation can also influence one other, making the drivers of lateral river migration a subject of persistent debate. One perspective argues that migration begins with outer bank erosion, causing local widening and the eventual deposition of sediment on the inner bank - a process termed "bank pull" (Van De Lageweg et al., 2014). In contrast,

https://doi.org/10.5194/egusphere-2026-4621
Preprint. Discussion started: 12 August 2026

another view suggests that migration starts with sediment accumulating on the inner bank, diverting flow and initiating outer bank erosion, a mechanism known as "bar push."

In this study, we analysed 4,923 river bends across a diverse range of rivers worldwide using 38 years of Landsat imagery to identify and assess bank pull and bar push processes. Erosion and sedimentation rates along each bankline were quantified by tracking variations in water indices through time in a pixel-based analysis. These rates of erosion and sedimentation were estimated using Google Earth Engine (GEE) and then analysed using Dynamic Cross-Correlation to determine process sequencing: whether erosion pulses precede sedimentation (indicating bank pull) or sedimentation pulses precede erosion (bar push). We also assessed our bank pull/bar push results in relation to a range of potential controlling environmental variables to explore the key factors influencing the mode of bend migration. With this approach, we address three fundamental questions: (i) Can satellite remote sensing combined with Dynamic Cross Correlation reliably identify bank pull and bar push mechanisms? (ii) Which process predominates worldwide, bank pull or bar push? and (iii) Which environmental factors influence the occurrence of each mechanism? This work represents the first quasi-global study of bank pull and bar push using remote sensing and cloud computing, providing a novel and robust approach to understanding this intriguing phenomenon.

2. Context

Meandering rivers migrate laterally across their floodplains through the combined action of outer bank erosion and inner bank sedimentation. Many numerical models describing river migration assume that outer bank erosion is directly influenced by the flow intensity, with inner bank sedimentation passively following to maintain a constant (through time) river width (Ikeda et al., 1981). This assumption is supported by long-term observations showing that, *on average* (our emphasis), river width remains relatively stable over extended periods (Lopez Dubon & Lanzoni, 2019). More recent studies, however, have shown that river width may fluctuate over time in response to changing environmental conditions, including variations in vegetation, hydroclimate, sediment supply, and the physical properties of the channel bed and banks (Akinola et al., 2019; Anderson et al., 2004; Chin, 2006; Francalanci et al., 2020). To address this complexity, researchers have developed models that separately quantify erosion and sedimentation dynamics (Darby et al., 2002; Darby et al., 2007; Eke et al., 2014; Langendoen et al., 2009). These models of transient width adjustment account for factors such as soil properties and vegetation on the outer bank, which influence erosion (Darby et al., 2002; Darby et al., 2007; Eke et al., 2014), as well as vegetation encroachment on the inner bank, which stabilizes point bars and promotes sediment deposition (Eke et al., 2014). Eke et al. (2014), for example, identified multiple modes of bank interaction, where the riverbanks on both sides of the bend can either erode simultaneously, undergo concurrent deposition, or exhibit asymmetrical migration patterns.

Nonetheless, in addition to being affected by the different environmental factors described above, erosion and sedimentation processes can also influence one other, creating complex interactions which numerical models fail to capture. Therefore, the drivers of lateral river migration remain a subject of debate. One perspective argues that migration begins with outer bank erosion, causing local widening and the eventual deposition of sediment on the inner bank - a process termed "bank pull" (Van De Lageweg et al., 2014). In contrast, another view suggests that migration starts with sediment accumulating on the inner bank, diverting flow and initiating outer bank erosion, a mechanism known as "bar push." A few previous researchers have tried to tackle the question of whether meanders migrate predominantly via bank pull or bar push, employing a variety of techniques including the use of computational models (Eke et al., 2014), physical experiments (Mahmoud et al., 2026; Van De Lageweg et al., 2014), as well as monitoring of bends using LiDAR deployed from drones (Martin et al., 2024) and other airborne platforms (Mason & Mohrig, 2018). Van De Lageweg et al. (2014) conducted a physical experiment with an artificial meandering river and identified bank pull as the dominant process. Mahmoud et al. (2026), on the other hand, using a 50-m-long sine-generated gravel-bed channel, found that the relative importance of bank-pull and bar-push varied through time and among bends, highlighting a range of complex morphodynamic behaviours.

Field studies using LiDAR have been conducted, but their scope remains limited. For example, Martin et al. (2024), using four years of drone-based LiDAR on a single river bend, found no consistent evidence of either bank pull or bar push dominance on the White River (USA). The authors explored bank pull and bar push mechanisms by analysing changes in river width, with river expansion indicating bank pull and narrowing suggesting bar push. However, they argued that because the White River has not reached width equilibrium over the past 55 years, neither process appears to be actively regulating its width. Mason and Mohrig (2018), in contrast, analysed 55 river bends over 4.5 years using airborne LiDAR data and found that, in the downstream reaches of the Trinity River (USA), bank pull was the dominant process of migration during flooding events due to increased erosion and limited point bar movement. Meanwhile, bar push was more prevalent in the upstream sections of the Trinity, where higher net deposition occurred. However, the

https://doi.org/10.5194/egusphere-2026-4621
Preprint. Discussion started: 12 August 2026

study by Mason and Mohrig (2018) discriminated the bank pull and bar push mechanisms based on an estimation of overall erosion and sedimentation rates combined with an assumption that higher erosion rates are associated with bank pull while higher sedimentation is linked to a dominance of bar push. Therefore, while the study by Martin et al. (2024) was spatially constrained to a single bend, Mason and Mohrig (2018) did not discretize outer-bank erosion and inner-bank sedimentation rates over time for direct comparison. The use of remote sensing time-series could address this limitation, enabling detailed detection of erosion and sedimentation over time across a large number of river bends. Such an approach could provide a more comprehensive understanding of the prevalence of bank pull versus bar push across diverse river systems.

Indeed, satellite technology has significantly enhanced our understanding of how river migration rates interact with factors such as vegetation, sediment load, flow discharge variability, and upstream sinuosity (Boothroyd et al., 2025; Constantine et al., 2014; Ielpi & Lapôtre, 2020; Leenman et al., 2023; Sylvester et al., 2019). These studies tend to simplify river analysis by extracting the river centreline, river width or static areas of erosion and sedimentation (Nagel et al., 2022). However, in natural environments, river width varies significantly with water levels, which fluctuate due to changing hydrological and climatic conditions (Feng et al., 2022; Phillips et al., 2024). This issue is particularly evident on the shallower inner bank, where even minor fluctuations in water level can cause substantial advance or retreat of the (water defined) shoreline. These changes can obscure bank pull and bar push signals, a challenge further amplified by the coarse resolution of some satellite imagery. To address this, a pixel-based analysis can be used to not only track long term trends of outer-bank erosion and inner-bank sedimentation (Nagel et al., 2025; Nagel et al., 2022), but also to determine their *timing*. This pixel-based approach, combined with methods to filter out short-term natural fluctuations, would provide a clearer identification of which bank (inner or outer) motion precedes or lags the other. Furthermore, a pixel-based analysis facilitates the detection of entire point bar formation and growth, which is important in evaluating bank pull and bar push mechanisms (Inoue et al., 2025; Van De Lageweg et al., 2014).

3. Methods

A total of 4,923 river bends from 64 rivers (wider than 55 m) worldwide were selected to analyse bank pull and bar push processes (Fig. 1a). The 55-meter width threshold corresponds to the minimum channel width necessary to accommodate a 30-meter resolution pixel, enabling the detection of rapidly migrating rivers, defined here as those exhibiting average lateral migration rates exceeding 3 meters per year. Rivers from 15 different Köppen climate regions, ranging from Tropical Rainforest to Cold Deserts, were included (Fig. 1b) to capture a broad range of environmental conditions. The selected rivers include examples from the Amazon Basin, such as the Juruá and Purus Rivers; rivers from arid Central Asia, such as the Ural and Syr Darya Rivers; and rivers from colder climates, such as Canada's Nelson River. All the analysed rivers are not affected by dams. Erosion and sedimentation analyses were conducted for each bend. To facilitate this, we created a polygonal boundary for each bend, delimited by its points of inflection. These polygons were manually drawn using the Water Transition Dataset as a reference (Nagel et al., 2025), which highlights areas of historical erosion and sedimentation (Fig. 1). Based on this information, we identified the points in time when riverbanks transition between erosion and sedimentation, characterizing the points of inflection. The methods are divided into three main elements: i) the estimation of erosion and sedimentation data using Landsat satellite imagery for each bend; ii) the processing of the erosion and sedimentation rates so-derived, using Dynamic Cross-Correlation to identify bends undergoing bank pull versus bar push processes, and; iii) performing correlations between the identified bank pull / bar push processes and selected environmental variables. All analyses and processing steps were applied to each river bend included in the study.

https://doi.org/10.5194/egusphere-2026-4621
Preprint. Discussion started: 12 August 2026

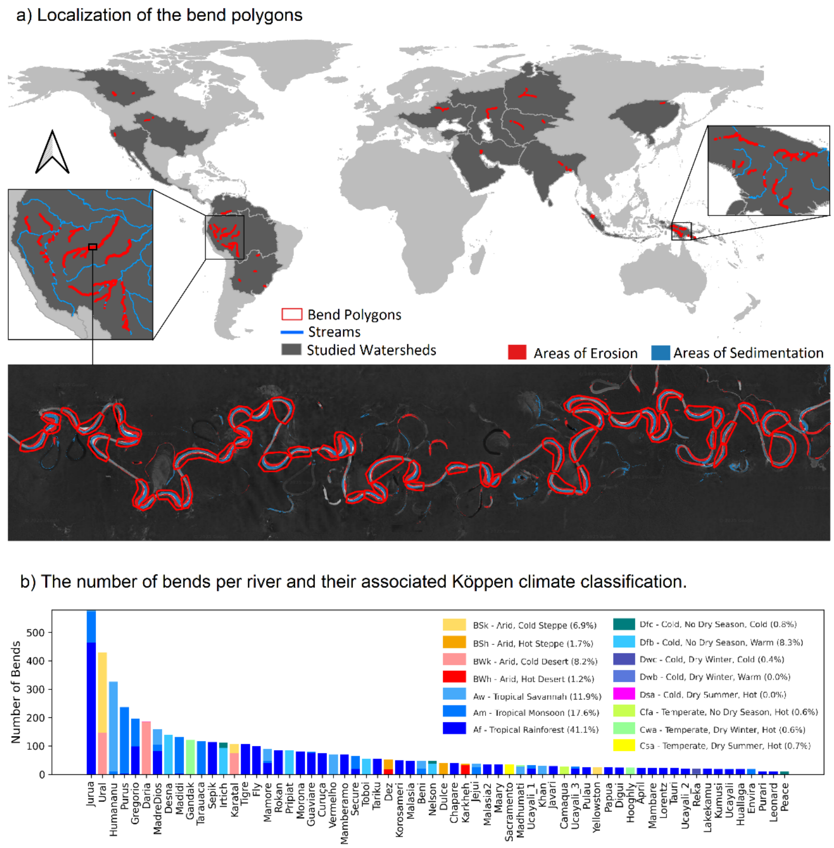

Figure 1 – (a) Locations of the 4,923 analysed river bends and (b) the number of bends per river, categorized by Köppen climate classification. The legend in panel (b) indicates the Köppen categories along with the percentage of total bends occurring in each.

3.1 Rates of erosion and sedimentation using remote sensing

Rates of lateral erosion and sedimentation were measured for each river bend using the cloud-based platform Google Earth Engine (GEE) and imagery from Landsat 5, 7, 8, and 9, spanning the period from 1984 to 2023. To achieve this, we first generated yearly median composites of the modified Normalized Difference Water Index (mNDWI), which uses a normalized difference between the green and mid-infrared band to identify surface water extent (SWIR) (Acharya et al., 2018; Chen et al., 2020; Deoli et al., 2022; Du et al., 2016; Gautam et al., 2015; Herndon et al., 2020; Rokni et al., 2014; Sarp & Ozcelik, 2017; Worden & de Beurs, 2020; Xu, 2006). These yearly median composites create images with little to no cloud interference and reduce the issue of seasonal width variability. To create the mNDWI yearly composites, the Fmask cloud mask included in the GEE image collection was used, and images with more than 50% cloud cover were excluded. However, even with yearly mNDWI composites, certain years lacked usable imagery due to persistent cloud cover. To address this, we applied a ±5-year median moving window, which filled data gaps and smoothed the dataset. This approach also mitigated rapid, non-permanent, fluctuations in river area and corrected image imperfections caused by undetected clouds, while maintaining the overall trend in relation to periods of identified erosion and sedimentation (Fig. 2a). Due to the use of median moving windows and data gaps in certain regions, the first five years of analysis were excluded, resulting in a 34-year analysis period.

https://doi.org/10.5194/egusphere-2026-4621
Preprint. Discussion started: 12 August 2026

Figure 2 illustrates our methodology for identifying periods of erosion and sedimentation within each bend polygon. Low mNDWI values indicate land, while high mNDWI values reflect the presence of water. As shown in Fig. 2a, the time series highlights three distinct cases: Point 1 demonstrates periods of increasing water extent due to riverbank erosion; Point 2 shows decreasing water extent due to sedimentation; while Point 3 exhibits both erosion and sedimentation over time. Point 3 is particularly noteworthy, as it highlights the dynamic nature of meandering rivers. Over the 39-year study period, the same location initially experienced outer-bank erosion but later transitioned to inner-bank sedimentation as the river shifted laterally. Therefore, our method captures the full range of processes, as some pixels experience only erosion, others only sedimentation, while some undergo both processes during the time period under consideration.

To identify the timings of erosion and sedimentation, we calculated a derivative within the 5-year moving window to detect altered trends in mNDWI. Increasing mNDWI trends indicate erosion, while decreasing trends indicate sedimentation (Fig. 2b). A threshold change in mNDWI was then applied to discriminate the periods of erosion and sedimentation: values exceeding 0.04 ΔmNDWI indicate erosion, while values below -0.04 ΔmNDWI signify sedimentation. The applied thresholds thus transform the continuous mNDWI trends into binary classifications of erosion and sedimentation (Fig. 2c). For each year, we summed all pixels within the bend polygon that experienced erosion or sedimentation to generate a time series for these processes. For example, in 2011 applying a threshold of 0.04 ΔmNDWI resulted in 255 pixels undergoing erosion and 163 pixels experiencing sedimentation (Fig. 2c).

To account for varying migration rates, we applied additional thresholds, including 0.06 ΔmNDWI for erosion and -0.06 ΔmNDWI for sedimentation, along with values of ±0.08, ±0.1, ±0.12, and ±0.14 ΔmNDWI. The final erosion and sedimentation rates were determined by calculating the median of all thresholds where more than half of the values were greater than zero. We ensured that the erosion and sedimentation thresholds were the same for each bend analysis. This approach ensured that only thresholds that effectively capture river movement were considered. Lower thresholds capture more subtle migrations but might generate greater noise related, for example, to atmospheric interference. Conversely, higher thresholds only capture faster migration patterns. Therefore, with this approach a balance between migration sensitivity and data quality is achieved. For instance, if the ±0.04, ±0.06, and ±0.08 thresholds successfully captured erosion and sedimentation rates while thresholds of ±0.1 and ±0.12 did not (having more than half of their values equal to zero), the final rates would be computed using the median rates of erosion and sedimentation captured using the ±0.04, ±0.06, and ±0.08 thresholds. This approach allowed for the detection of modest sub-pixel shifts, addressing one of the primary previous limitations of using Landsat imagery for geomorphological studies; its 30-meter spatial resolution. Considering all thresholds applied and the total of 4,923 bends, a total of 1,004,292 rates of erosion and sedimentation were estimated (4,923 bends x 34 years x 6 different thresholds), a large dataset that was crucial for the systematic detection of bank pull and bar push.

https://doi.org/10.5194/egusphere-2026-4621
Preprint. Discussion started: 12 August 2026

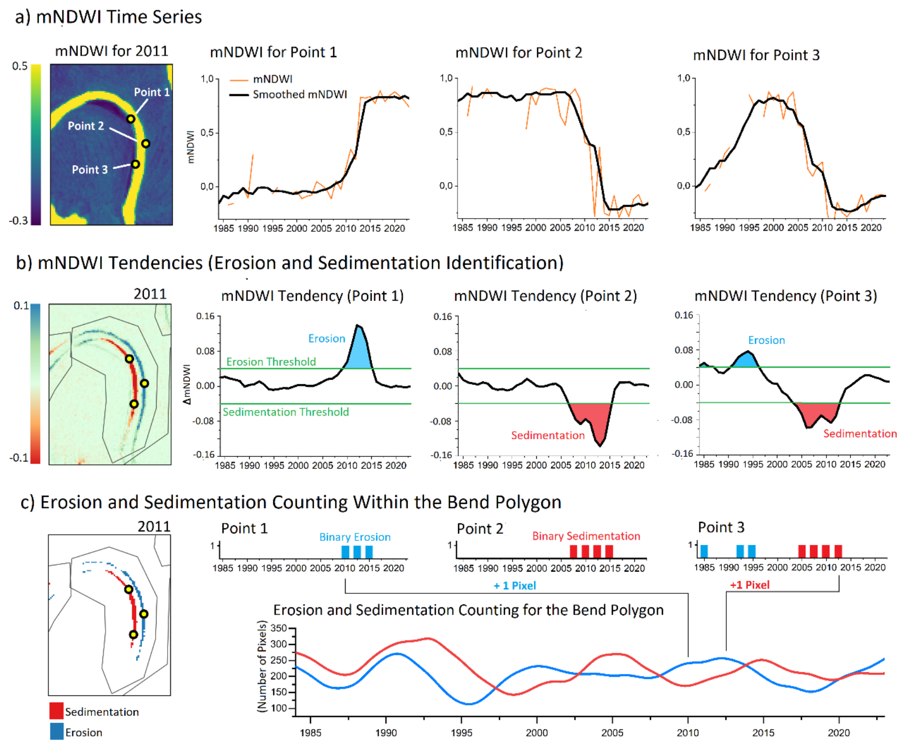

Figure 2 – A flowchart illustrating the methodology for detecting erosion and sedimentation rates at individual river bends. The diagram delineates (a) the temporal variations of the modified Normalized Difference Water Index (mNDWI) at three distinct points, (b) the mNDWI trends over time, incorporating predefined erosion and sedimentation thresholds, and (c) the identification of erosion and sedimentation periods, along with the quantification of these processes within the specified bend polygon.

Figure 3 illustrates the main concept behind the methodology. The upper panel shows the temporal evolution of mNDWI values derived from satellite imagery, while the lower panel presents the corresponding detrended rates of erosion and sedimentation for an example bend. Although the workflow involves multiple processing steps, the underlying principle is straightforward: long-term changes in water occurrence are used to quantify riverbank erosion and sediment deposition from satellite observations.

https://doi.org/10.5194/egusphere-2026-4621
Preprint. Discussion started: 12 August 2026

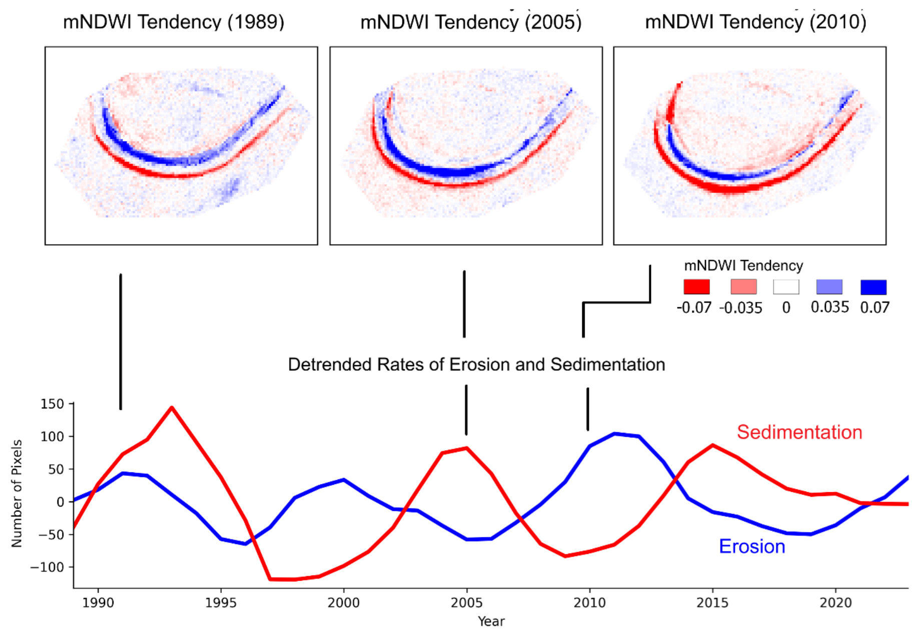

Figure 3 - Example of mNDWI tendency maps for 1991, 2005, and 2019 (top), and the corresponding detrended erosion and sedimentation time series (bottom) for a representative river bend.

3.2 Bank pull and bar push identification

The rates of outer-bank erosion and inner-bank sedimentation were compared using Dynamic Cross-Correlation. We first detrended the rates of erosion and sedimentation, using the python package scipy.signal, to focus on the analysis of fluctuations of both processes, and we excluded the first 5 years of analysis to reduce noisiness, creating a time series covering the period from 1989 to 2023. We then correlated the outer-bank erosion and inner-bank sedimentation rates for every bend introducing various time lags for erosion. For each time lag, we calculated and recorded the correlation coefficient, which indicates the strength and direction of the relationship between the two processes at different temporal offsets. We then selected the time lag associated with the highest positive correlation (but only if the condition $R > 0.7$ was met), to retain time lags with ‘strong’ (Ratner, 2009) correlations. A negative time lag indicates that outer-bank erosion precedes inner-bank sedimentation, thereby identifying bank pull, while a positive time lag indicates that sedimentation precedes erosion, characterizing bar push. This method was applied using a 10-year moving window, allowing us to track changes in time lags between outer-bank erosion and inner-bank sedimentation. A maximum lag of 5 years was set, generating a time series of lags for each bend. To remove outliers, lags that did not persist for more than 3 consecutive years were excluded. A total of 19,383 out of 121,204 lags (16.0%) were excluded based on this criterion. Based on the resulting lag time series, we classified each bend according to its dominant process. Bends with consistently negative lags were classified as bank pull dominated, while those with consistently positive lags were identified as undergoing bar push. Bends showing no lag were categorized as having Similar Rates. Bends that alternated between bank pull and bar push were classified as Undetermined.

To identify switching behaviour, where a bend initially dominated by bank pull transitions to bar push or vice versa, we selected bends with only a single transition: either bank pull at the beginning that shifts to bar push, or an initial state of bar push that shifts to bank pull. Bends that switched more than once were excluded, as they represent complex behaviour. Additionally, a bend exhibiting switching behaviour must show two consecutive pulses of erosion (for a transition from bar push to bank pull) or two consecutive pulses of sedimentation (for a transition from bank pull to bar push), deviating from the typical pattern of alternating erosion and sedimentation pulses. To detect these pulses, we used the scipy.signal.find_peaks function in Python. Based on this approach, bends classified as undergoing switching processes were

https://doi.org/10.5194/egusphere-2026-4621
Preprint. Discussion started: 12 August 2026

categorized as: i) Push-to-Pull – when the Dynamic Cross-Correlation indicates a transition from bar push to bank pull over time and there are two consecutive peak pulses of erosion, and; ii) Pull-to-Push – when the Dynamic Cross-Correlation indicates a transition from bank pull to bar push over time and there are two consecutive pulses of sedimentation.

3.3 Environmental variables controlling bank pull versus bar push

To identify potential factors influencing bank pull or bar push, we collected a range of pertinent environmental data for each bend. The environmental factors we considered in this analysis included climatic conditions (Köppen climatic environments, temperature), surface soil characteristics (e.g., clay, silt, coarse fragments, bulk density, and organic carbon content), and various river hydromorphology metrics (slope, sinuosity, radius of curvature, width, discharge, suspended sediment load, bedload proportion, and bedload). Additionally, catchment topographic data (elevation) and land cover information (vegetation) were also incorporated. The source of each of the data sets representing these variables is summarised in Table 1. The role of riparian vegetation was assessed using the Enhanced Vegetation Index (EVI) calculated from MODIS, which ranges from 0 (indicating no vegetation) to 1 (representing dense vegetation). The radius of curvature was measured along the river centreline by calculating the mean angular change between consecutive points and computing the inverse of the resulting curvature.

Table 1 – Environmental variables used in the multivariable binary logistic regression analysis.

Variable	Range (min and max)	Transformation for every bend	Source
Temperature (Celsius)	(-5.1 - 27.5)	Mean Temperature from 1984 to 2023	(Hersbach et al., 2024)
Köppen Climatic Classification	(Discrete classes)	Köppen class that intersects with the bend polygon	(Kottek et al., 2006)
Clay (g/kg) Sand (g/kg) Silt (g/kg), Organic Carbon Content (dg/kg), Coarse Fragments (cm^3/dm^3), Bulk Density (cg/cm^3)	(102 - 484) (70 - 662) (162 - 655) (81 - 2133) (0.2 - 212) (62- 153)	Mean value within each bend polygon	(Poggio et al., 2021)
Width (m)	(42 – 601)	Median value of all temporal width measurements from transects located within the bend polygon	(Allen & Pavelsky, 2018)
Discharge (m^3/s)	(0.004 - 8084)	Mean long-term discharge (1971–2000)	(Linke et al., 2019)
Slope (m/km)	(0 – 6.98)	Slope of the river section that intersects the bend polygon. The sinuosity is the ratio of total reach length to the straight-line distance between reach endpoints	(Altenau et al., 2021)
Radius of Curvature (m)	(5.2 - 213,959,849)	Curvature calculated by extracting the river section from Altenau et al. (2021)	(Altenau et al., 2021)
Suspended Sediment Load (Kg/s), Bedload Proportion (%), Bedload (Kg/s),	(0.24 - 82190) (0.1 - 74.2) (0.002 - 67.9)	Parameters represent the average between 1990-2019, selected according to the minimum distance between the bend polygon and the river line from Cohen et al. (2022)	(Cohen et al., 2022)
Vegetation	(0.095 – 0.62)	Temporal mean Enhanced Vegetation Index (EVI), excluding water areas, within each bend polygon	(Jarchow, 2019)

https://doi.org/10.5194/egusphere-2026-4621
Preprint. Discussion started: 12 August 2026

From the collected variables, we derived the unit discharge, defined as the ratio of river discharge to channel width (Equation 1). Higher values of this index indicate conditions where greater discharge is constrained within narrower channels, implying higher flow intensity per unit width. This formulation is consistent with the relationship between discharge, velocity, and cross-sectional area (V = Q / A), where increased discharge per unit width is expected to correspond to higher flow velocities.

$$Unit\ discharge = \frac{Discharge\ (m^3/s)}{River\ Width\ (m)} \tag{1}$$

We conducted a multivariable binary logistic regression analysis using the Python package *statsmodels* to examine the relationship between bend migration mechanism (bank pull or bar push) and a set of environmental variables. The dependent variable was defined as a binary classification of each bend (bank pull = 1; bar push = 0), while the explanatory variables included unit discharge, vegetation, soil sand content, and soil bulk density. The logistic regression was performed at the bend scale to evaluate how these environmental characteristics influence the likelihood of a bend being classified as bank pull rather than bar push. Model coefficients were estimated using maximum likelihood, and odds ratios were calculated to quantify the magnitude and direction of the association between each explanatory variable and the probability of bank pull occurrence.

4. Results

4.1 Comparison of erosion and sedimentation rates with river migration data

To lend confidence to our analysis, we initially benchmark our estimates of pixel-scale erosion and sedimentation rates against channel migration rates estimated independently by Langhorst and Pavelsky (2023). The total count of erosion and sedimentation pixels detected by our method, summed from 1984 to 2023 within each bend polygon, correlates well with the corresponding migration rates as estimated by Langhorst and Pavelsky (2023). Both relationships followed a power law, becoming approximately linear after log–log transformation ($R^2 = 0.71$ for erosion and $R^2 = 0.64$ for sedimentation; Fig. 4a). While our method is designed to adaptively capture intra-bend erosion and sedimentation rates with precision using variable thresholds, rather than directly comparing rates between bends, the alignment of our data with the migration rates estimated by Langhorst and Pavelsky (2023) suggests that our method can reliably detect migration dynamics. Moreover, the comparison illustrates the sensitivity of the method when dealing with higher combined migration rates. This greater sensitivity is derived from the use of the adaptative threshold approach to detect different rates of migration, as described in the methods. As migration rates increase, higher (for erosion) and negatively lower (for sedimentation) thresholds are required to accurately detect rivers with fast migration rates (Fig 4b). For instance, when the erosion migration rate is 1.74 m/yr, the maximum threshold required is typically 0.04 ΔmNDWI. In contrast, for a faster erosion migration rate of 10.9 m/yr, the required threshold increases to 0.14 ΔmNDWI. When the erosion migration rate exceeds 20 m/yr, the maximum threshold of 0.14 ΔmNDWI dominates (Fig 4b). A similar pattern is observed in the sedimentation threshold behaviour. With this approach, our method adapts to capture migration rates ranging from subtle to rapid river motions.

https://doi.org/10.5194/egusphere-2026-4621
Preprint. Discussion started: 12 August 2026

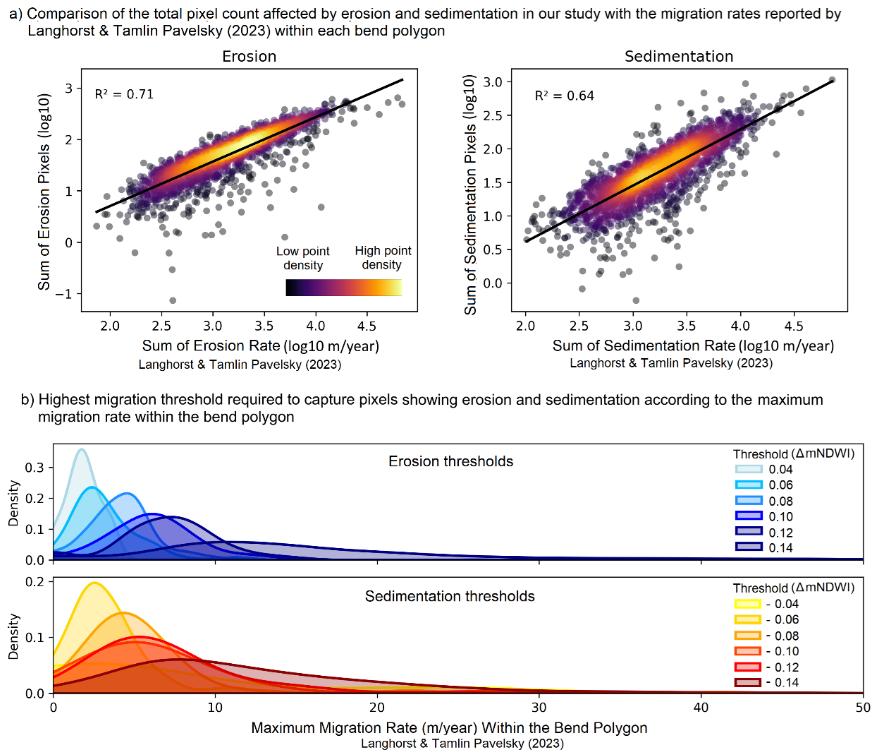

Figure 4 – (a) Comparison between total erosion and sedimentation pixels as derived from the methods employed herein and the sum of migration rates within each bend polygon. (b) Highest migration threshold required to detect pixels undergoing erosion and sedimentation, based on the maximum migration rate within each bend polygon. Analysis includes a total of 2,000 bends, with migration rates sourced from Langhorst and Pavelsky (2023).

4.2 Overall frequency of bank pull versus bar push

Fig. 5 presents four examples of bend polygons, illustrating their computed erosion and sedimentation rates over time (after detrending the rates of erosion and sedimentation). Below each graph, the lag with the highest correlation (from the Dynamic Cross-Correlation analysis) is also indicated. For example, the bend in Fig. 5a exhibits episodes of erosion that precede sedimentation, indicating bank pull, with lags of -2 years between 1989 and 1994, and -4 years during both of the periods 1999 to 2006 and 2011 to 2016. The Dynamic Cross-Correlation method also identifies bar push in Fig. 5b, with lags of +1, +3, and +4 years. In contrast, Fig. 5c shows similar rates of erosion and sedimentation over time, with the best fit lag being 0 years (no lag). The sporadic bank pull and bar push lags detected in Fig. 5c were excluded, as they did not persist for three or more consecutive years. Fig. 5d illustrates a complex interaction between erosion and sedimentation, where a sequence of erosion followed by sedimentation, characteristic of bank pull dynamics, is interrupted by two consecutive phases of sedimentation. This disruption, detected through the Dynamic Cross-Correlation and the consecutive peaks, indicates a shift from bank pull to bar push behaviour.

https://doi.org/10.5194/egusphere-2026-4621
Preprint. Discussion started: 12 August 2026

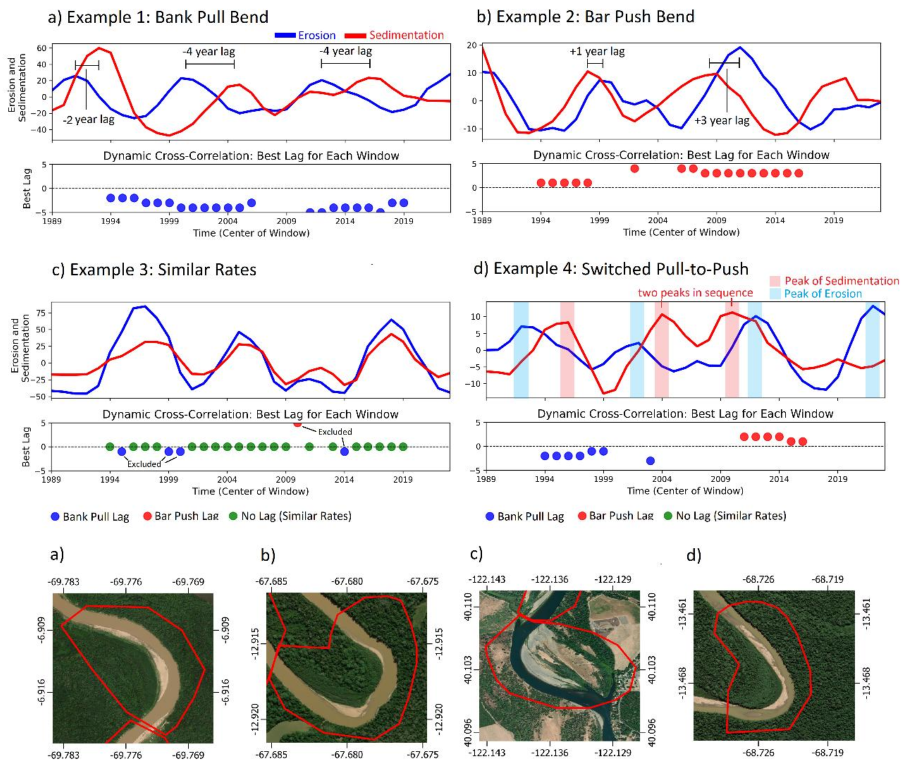

Figure 5 – Erosion and sedimentation rates with Dynamic Cross-Correlation results for four example bends, illustrating the locations of polygon bends classified as having lateral migration dominated by (a) bank pull, (b) bar push, (c) similar rates (i.e. no doiminant mechanism) and (d) a transition from pull to push.

Out of the 4,923 original river bends, 1,005 (20.4%) were classified as migrating via bank pull with 792 (16.1%) migrating via bar push, with the majority (3,126 bends, 63.5% of the total) not exhibiting any clear signal. This means that, of those bends where a clear signal was identified, 56% and 44% exhibited pull and push behaviour, respectively (Fig. 6a). Of the 3,126 bends that exhibited no dominant bank pull or bar push signal, 15 bends (0.3% of the total sample of 4,923 bends) experienced similar rates of erosion and sedimentation, with switching behaviours evident at 133 bends (2.7%), whilst 2,978 bends (60.5%) had patterns too complex to classify. Despite the large overall number of unclassified bends, those with identifiable patterns displayed clear signals of bank pull and bar push. The number of clearly classified bends (1,797, representing 36.5% of all bends) was sufficient to reveal spatial patterns in these processes across different rivers and regions (Fig. 6a). For example, the tributary of the Ucayali River, labelled as Ucayali-Trib 1 in Figure 6b, is a relatively small Amazonian river with a width of approximately 100 meters. All of its identifiable river bends were classified as undergoing bar push (Fig. 6b). The Orthon River (another Amazonian tributary) has 61% of its identifiable bends classified as bar push and 39% as bank pull (Figure 6b). This pattern is reversed in the Ural River, Centra Asia, with 73% of its bends classified as migrating via bank pull, versus just 27% as bar push. However, one of the most intriguing patterns is observed on the Juruá River. While the river as a whole shows a relatively balanced distribution of 52% bar push and 48% bank pull migrating bends, a notable process shift occurs downstream of its confluence with the Tarauacá River. In this downstream reach, which has a notably higher proportion of fine sediments in its boundary materials (see below), the Juruá transitions into a sequence of predominantly bank pull migrating bends, aligning more closely with the results from the Tarauacá River itself, where 100% of the bends are classified as migrating via bank pull. Potential causes for the contrasting behaviours of the Tarauacá and Jurua rivers are explored in Section 3.3. This suggests that river bends and their characteristics are interconnected, with one section potentially influencing the behaviour of downstream segments.

https://doi.org/10.5194/egusphere-2026-4621
Preprint. Discussion started: 12 August 2026

Another important observation is that most bar-push dominated rivers are located in tropical environments, particularly within the Amazon Basin, as classified by the Köppen climate system (Kottek et al., 2006) (Figure 6c). These environments encompass the Tropical Rainforest (Af), Tropical Monsoon (Am), and Tropical Savannah (Aw) climate classes, all of which are characterized by high annual temperatures (consistently above 18 °C) and substantial precipitation. This combination fosters the development of dense riparian vegetation, which can influence channel morphology (Ielpi & Lapôtre, 2020). In contrast, bank-pull dominated rivers tend to be more prevalent in arid, temperate, and cold climate zones, which are typically regions with lower vegetation density. These regions span a wide range of environmental conditions, from dry deserts and steppes (e.g., BWh, BWk, BSh, BSk) to seasonally variable temperate zones (e.g., Csa, Cfa, Cwa) and colder continental climates (e.g., Dwb, Dwc, Dfc, Dfb). Altogether, this distribution pattern highlights the role of climatic and environmental conditions in modulating river morphodynamics, particularly the balance between bank-pull and bar-push mechanisms, a relationship that is also explored in greater detail in Section 3.3.

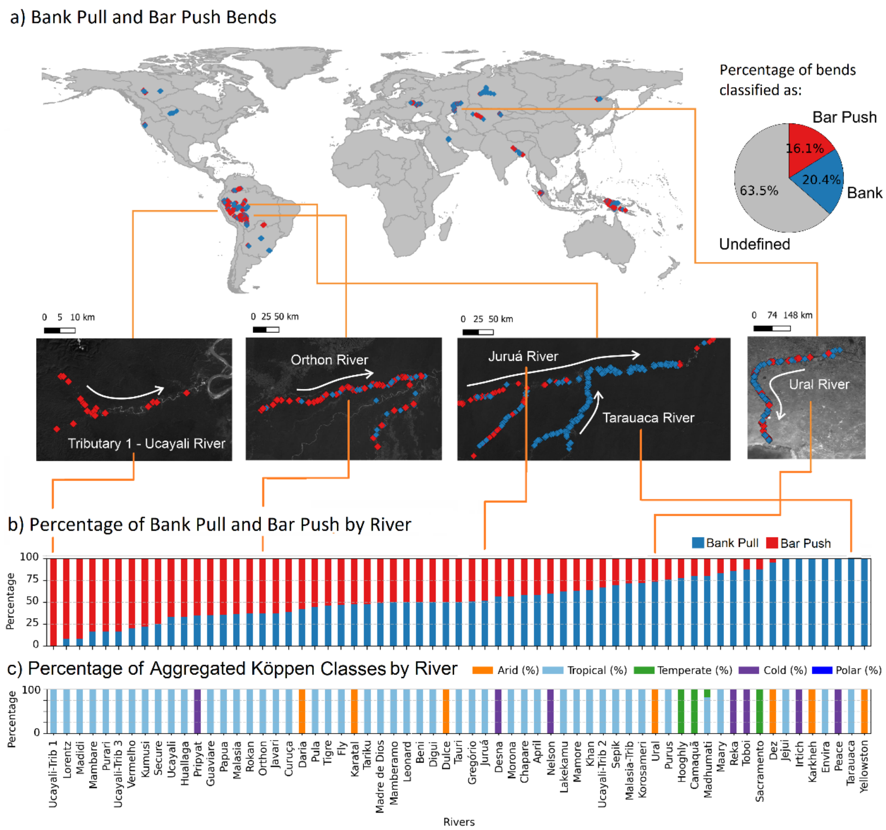

Figure 6 – Proportions of bends classified as (a) bank pull (blue) or bar push (red), (b) the analysed rivers and their percentage distributions and (c) their corresponding Köppen classification.

4.3 Environmental factors driving bank pull versus bar push

To identify the environmental factors that potentially influence the occurrence of bank pull versus bar push, a multivariable logistic regression was conducted, using the presence of bar push (1) versus bank pull (0) as the dependent variable, and a set of hydrological, sedimentary, and vegetative descriptors as independent variables. The analysis was based on 1,570 observations classified as either bank pull or bar push dominant for which environmental variables were available. It should be noted that here the number of analyzed bends (1,570) is therefore lower than the total number of pull or push-dominant bends (1,797) because

https://doi.org/10.5194/egusphere-2026-4621
Preprint. Discussion started: 12 August 2026

environmental data were not available for all bends. From the full set of predictors evaluated, the final model retained four statistically significant variables: vegetation density ($p < 0.001$), sand content ($p < 0.001$), bulk density ($p < 0.001$), and the unit discharge ($p < 0.01$). Vegetation density showed a strong positive association with the occurrence of bar push, whereas unit discharge exhibited a significant negative relationship, indicating that higher flow power conditions tend to favour bank pull. Sand content and bulk density both showed positive relationships with bar push. The resulting logistic regression model is statistically significant (Likelihood Ratio Test, LLR, $p < 0.001$), with a McFadden pseudo-R^2 of 0.038 and an Area Under the Receiver Operating Characteristic Curve (AUC) of 0.64. Variance Inflation Factor (VIF) diagnostics confirmed low interdependence among predictors (VIF < 1.2 for all variables). These results are intended for inferential purposes rather than predictive modelling, with the aim to identify statistically supported relationships between environmental variables and channel response mechanisms. They therefore reflect associations within a complex and stochastic geomorphic system, rather than a deterministic or predictive framework.

As described in the methodology, vegetation density is represented by the mean Enhanced Vegetation Index (EVI) within each bend, derived from MODIS imagery. EVI is a unitless index ranging approximately from 0 to 1, where higher values indicate denser and more vigorous vegetation, and lower values the converse. Unit discharge represents the mean annual river discharge normalized by channel width ($m^3\ s^{-1}\ m^{-1}$), serving as a proxy for flow intensity. Sand content was derived from the average proportion of sand in the soil within each bend ($g\ kg^{-1}$). Bulk density, expressed in $cg\ cm^{-3}$, represents the dry mass of soil per unit volume and is an indicator of soil compaction, with higher values generally corresponding to denser, more compact soils. While vegetation density, sand content, and bulk density characterize local conditions within each river bend, unit discharge represents a hydraulic property of the river system.

Table 2 – Summary of multivariable binary logistic regression results for the percentage of bank pull in each river. Positive coefficients increase the chance of bar push, while negative coefficients increase the chance of bank pull.

Variable	Coefficient	Standard Error	z	p-value
Intercept	-4.82	0.772	-6.253	0.000
Vegetation (EVI)	3.68	0.557	6.606	0.000
Unit Discharge ($m^3\ s^{-1}\ m^{-1}$)	-0.0392	0.014	-2.776	0.006
Sand Content ($g\ kg^{-1}$)	0.003	0.001	5.224	0.000
Bulk Density ($cg\ cm^{-3}$)	0.018	0.005	3.410	0.001

https://doi.org/10.5194/egusphere-2026-4621
Preprint. Discussion started: 12 August 2026

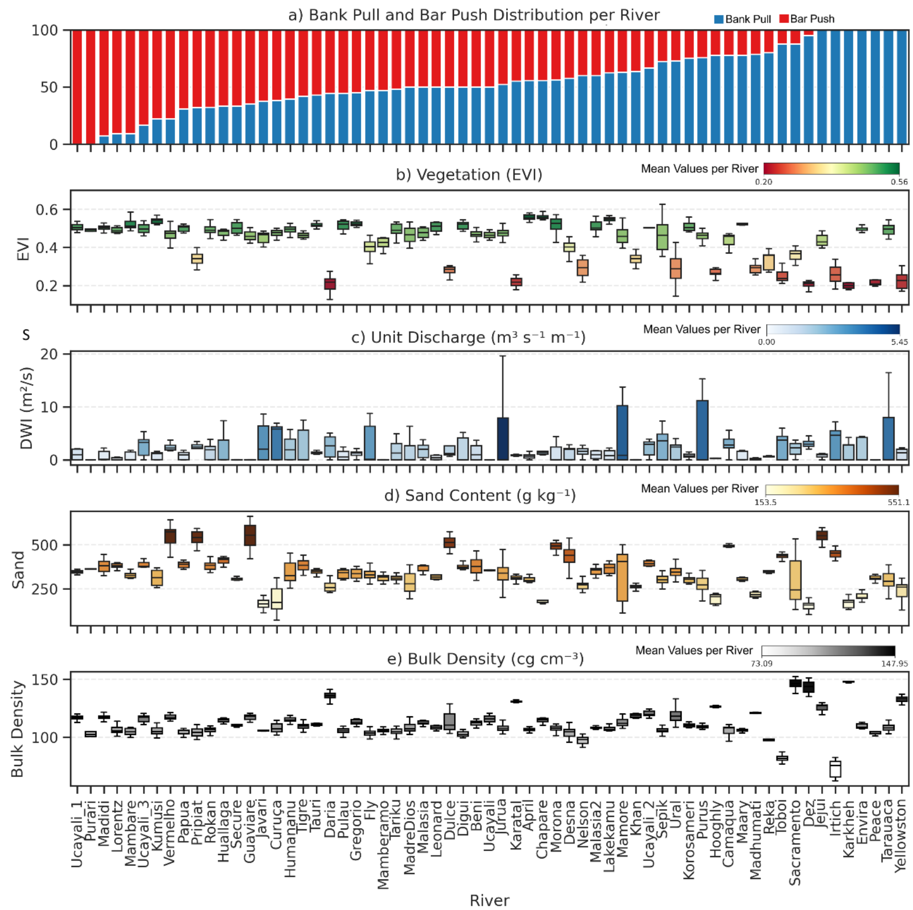

Figure 7 – (a) Frequency of occurrence of bank pull versus bar push for each river, with corresponding mean river values of (b) the vegetation density (EVI), (c) unit discharge (DWI), (d) sand content and (e) bulk density.

The regression model results show that the presence and density of riparian vegetation negatively impacts the percentage of bends migrating via bank pull, meaning that rivers with less vegetation are more likely to experience bank pull during channel migration. This likely happens because the absence of vegetation reduces bank stability, facilitating erosion of the outer bank. In contrast, vegetated rivers tend to have more erosion-resistant banks (Finotello et al., 2024). Erosion in these rivers with higher bank resistance might occur only after sediment accumulates along the inner bank, eventually pushing the river channel outward, a characteristic of the bar push mechanism of lateral channel migration. Among the five rivers with the highest bank pull percentages (the Toboi River in Russia (88.0%), the Dez River in Iran (90.9%), the Irtich River in Russia (100%), the Tarauacá River in Brazil (100%), and the Yellowstone River in the USA (100%) (Figure 7a), only the Tarauacá River is highly vegetated, with a mean EVI of 0.49 (Figure 7b). In contrast, the remaining four rivers with high bank pull percentages have EVI values below 0.24 (Figure 7b).

The unit discharge is positively associated with the prevalence of bank pull (Table 2). Elevated unit discharge values reflect more energetic flow conditions concentrated within narrower channels, which favour outer-bank erosion and, consequently, bank pull. The high unit discharges of the Amazonian Tarauaca and Purus River (4.06 and 4.26 m^2/s, respectively) might explain why those rivers are dominated by bank pull even though they are surrounded by dense forests (Figure 7c). In contrast, the 11 rivers with the highest bar push percentages all have unit discharge values lower than 2.65 m^2/s (Figure 7c).

https://doi.org/10.5194/egusphere-2026-4621
Preprint. Discussion started: 12 August 2026

Sand is an important variable positively associated with the bar push mechanism (Table 2). Point bars are primarily composed of sand- and gravel-sized sediments (Van De Lageweg et al., 2014), which are preferentially deposited on the inner bank of meander bends. Consequently, rivers with higher sand availability tend to develop more efficient lateral accretion processes, promoting point bar growth and enhancing the bar push mechanism. Soil bulk density, defined as the dry mass of soil per unit total volume, reflects the degree of soil compaction and is inversely related to porosity and erodibility (McNabb et al., 2001). Higher bulk density values therefore indicate more mechanically resistant banks, reducing the likelihood of outer-bank erosion. This potentially favours inner-bank deposition and bar growth, thereby reinforcing the bar push mechanism (Jepsen et al., 1997). Overall, our results suggest that bar push is favoured in settings characterised by strong banks, sufficient sand supply for bar construction, and comparatively lower hydraulic energy. In contrast, bank pull tends to dominate in systems with more erodible banks and more energetic flow conditions, which enhance outer-bank erosion.

Discussion

By analysing a 39-year time series of satellite imagery from 4,923 river bends worldwide, we have systematically identified, for the first time, river bends shaped by bank pull and bar push processes in real environments. Our results therefore provide a positive answer to the first question posed in this study: satellite remote sensing combined with Dynamic Cross Correlation can reliably identify bank pull and bar push mechanisms. Our large-scale dataset revealed that both mechanisms of lateral channel migration occur across diverse environments. However, most of the bends (63.5%) in our analysis have no clear signal of bank pull or bar push over time. This finding is consistent with the recent study Mahmoud et al. (2026), who demonstrated in a 50-m-long experimental meandering channel that bank-pull and bar-push mechanisms frequently alternate through time and between bends of the same river, making it challenging to identify conditions under which either mechanism dominates. Our results complement Mahmoud et al. (2026) by highlighting that this natural variability is also widespread in natural river systems across a broad range of environmental settings, helping to explain the predominance of the "no clear signal" class in our classification. Understanding the processes driving these transitions represents an important avenue for future research. Although bends exhibiting transitions between mechanisms were also identified, the scale of our analysis allowed us to focus on bends with a persistent and clearly expressed migration style. By concentrating on bends with stronger bank-pull or bar-push signatures, we were able to more robustly evaluate their relationships with environmental variables. This approach reduces the ambiguity arising from the simultaneous interaction of erosion and deposition processes, a challenge that has frequently complicated the interpretation of natural river systems (Martin et al., 2024; Mason & Mohrig, 2018).

While both lateral channel migration mechanisms occur in natural environments, we found that their relative dominance is influenced by vegetation density, flow, and soil characteristics. Specifically, the presence of dense vegetation, a low unit, high sand availability and higher soil bulk density all favour bar push. In contrast, rivers in sparsely-vegetated environments, with high unit discharge, low sand availability and low bulk density are more likely to be dominated by bank pull. The dominance of the influence of vegetation is reflected in our finding that, when aggregated to the scale of rivers, rivers with the highest frequency of occurrence of bar push migrating bends (>66%) are located in Köppen-classified tropical climates, regions typically characterized by dense forests. In contrast, for rivers exhibiting the highest bank-pull percentages; such as the Toboi River (Russia; 88.0%), Dez River (Iran; 90.9%), Irtysh River (Russia; 100%) and Yellowstone River (USA; 100%) are all situated in sparsely or non-vegetated environments.

The importance of vegetation density in controlling the relative frequency of bar push versus bank pull migration is interpreted to reflect how the presence of vegetation enhances bank stability (Finotello et al., 2024; Krzeminska et al., 2019; van Dijk et al., 2013; Zhu et al., 2022). Consequently, in vegetated rivers, erosion tends to occurs only after point bars have grown sufficiently to redirect river flow toward the vegetated outer bank (Inoue et al., 2025). Additionally, vegetation stabilizes and traps sediments at the inner bank (Braudrick et al., 2009), promoting point bar growth over time (Bywater-Reyes et al., 2018). The fall of trees into the river due to bank erosion can also contribute to bar push, since it blocks the river and therefore slow sediment transport, potentially further enhancing deposition and point bar development (Galia et al., 2024). In contrast, non-vegetated rivers are more susceptible to erosion, making bank pull the more likely dominant process. A similar pattern was observed by Van De Lageweg et al. (2014), who reported a dominant bank pull response in experimentally formed meandering rivers devoid of vegetation. Therefore, although vegetation is well understood as being an important factor for controlling erosion and point bar growth (Abernethy & Rutherfurd, 2000; Eke et al., 2014; Simon & Collison, 2002), our research is the first to identify a correlation between vegetation density and the relative prevalence of bank pull and bar push.

https://doi.org/10.5194/egusphere-2026-4621
Preprint. Discussion started: 12 August 2026

Soil properties also influence the relative dominance of bank pull and bar push. Higher soil bulk density increases bank resistance to fluvial erosion (Jepsen et al., 1997), favouring conditions in which channel migration occurs primarily through the gradual growth of point bars rather than through direct outer-bank retreat. Under these conditions, bank erosion is more likely to be delayed until point-bar accretion becomes sufficiently large to displace the channel laterally. However, sustained point-bar growth also requires an adequate supply of sand, which constitutes a major component of point-bar deposits (Van De Lageweg et al., 2014). Consistent with this mechanism, greater sand availability was associated with a higher prevalence of bar push in our analysis. By contrast, sediment load metrics, such as bedload and suspended sediment concentrations, were not significantly associated with migration mechanism, contrary to theoretical expectations (Eke et al., 2014). A possible explanation is that globally available sediment datasets are spatially coarse, heavily interpolated, and unable to capture the local variability in sediment supply at the bend scale. By contrast, the sand variable may partly capture the local availability of sediment suitable for point-bar construction, even if it does not directly represent sediment flux through the river system. Furthermore, bar push was most prevalent in densely vegetated rivers with relatively low unit discharges, conditions that favour sediment retention and point-bar stability. Vegetation enhances sediment trapping and reduces local flow velocities (Bywater-Reyes et al., 2018; Galia et al., 2024), promoting bar growth even without exceptionally high sediment inputs. Future studies integrating bend-scale sediment budgets with direct sediment transport measurements are needed to disentangle the relative roles of sediment supply, storage, and retention in controlling meander migration mechanisms.

It is important to emphasize that the purpose of the Logit model employed here was to identify environmental variables statistically associated with the occurrence of bank-pull and bar-push migration, rather than to provide a predictive framework. The low predictive performance of the derived model suggests that additional local controls, which are difficult to quantify consistently at a global scale, likely also influence the dominant migration mechanism. This interpretation is consistent with Mahmoud et al. (2026), who demonstrated that identical flow forcings can still produce markedly different push versus pull responses depending on local bend-scale boundary conditions. Consequently, while the variables identified here reveal broad environmental tendencies associated with bank-pull and bar-push migration, a substantial proportion of the observed variability is governed by local geomorphic and hydraulic factors. With the assessment of the overall environmental interactions to produce bank pull and bar push, our findings have implications for meander migration modelling. Most numerical models of meander migration implicitly assume that bends migrate primarily through bank pull processes; i.e., that outer bank erosion initiates channel movement, with inner bank deposition responding passively to preserve channel width (Ikeda et al., 1981; Parker et al., 2011). Although bank pull is the most common persistent mechanism, its dominance is modest. Among bends showing a clear migration style, 20.4% were classified as bank pull and 16.1% as bar push, whereas approximately 64% exhibited no persistent temporal lead–lag relationship. These findings indicate that neither mechanism universally dominates meander migration, and that alternating or synchronous behaviour is the prevailing pattern in natural rivers. This suggests that the idealised conceptual dichotomy of pull versus push does not capture the full range of meander dynamics occurring in natural systems. Particularly in tropical river environments, where bar push dominates and inner bank processes are more prevalent, existing meander migration models may require refinement to account for cases where sedimentation leads rather than follows erosion. Thus, we advocate for a re-evaluation of migration modelling frameworks, especially those applied to densely vegetated tropical rivers, to incorporate bar push as a legitimate and potentially co-dominant mechanism.

Conclusion

Our study demonstrates that, overall, bank pull migrating bends occur slightly more frequently (56%) than those migrating through bar push (44%), with both types of bend migration process observed across a wide range of natural river environments. However, our findings do reveal subtle patterns in the relative frequency of push versus pull migrating bends based on river characteristics. Densely vegetated rivers with slower flow and finer (more resistant) boundary materials are more likely to exhibit migration via bar push, where sediment deposition along the inner bank plays a dominant role. In contrast, less densely vegetated rivers with faster flows and with coarser boundary materials, show a higher occurrence of bends migrating via bank pull. This means that the rivers with the highest proportion of bar-push migration in our dataset are predominantly located in densely vegetated tropical environments. Among the 64 rivers analysed, 11 of the most bar-push dominated rivers are classified as tropical. These results contribute to a better understanding of meandering river dynamics, highlighting the influence of vegetation, bank material characteristics, and unit discharge in determining bend migration processes. Beyond these geomorphic insights, the remote sensing framework developed here provides a scalable approach for investigating

https://doi.org/10.5194/egusphere-2026-4621
Preprint. Discussion started: 12 August 2026

temporal interactions between erosion and deposition across large river networks. Its application is not restricted to distinguishing bank pull and bar push, but could also support studies of channel adjustment under changing climate, altered sediment supply, dam regulation, and river restoration, where understanding the coupling between erosion and deposition is essential.

Acknowledgement

This work was undertaken as part of GN's PhD studies which were supported by a studentship within the INSPIRE Doctoral Training Programme (DTP) funded by the Natural Environmental Research Council [grant number NE/S007210/1]

Author contribution: GN, SD, JL and EL conceptualized the research goals and aims; GN developed the design of methodology, created the published work and applied statistical, mathematical and computational techniques to analyse or synthesize study data; SD, JL and EL performed critical reviewing and revision.

References

Abernethy, B., & Rutherfurd, I. (2000). The Effect of Riparian Tree Roots on the Mass-Stability of Riverbanks. *Earth Surface Processes and Landforms*, *25*, 921–937. https://doi.org/10.1002/1096-9837(200008)25:9<921::AID-ESP93>3.0.CO;2-7

Acharya, T. D., Subedi, A., & Lee, D. H. (2018). Evaluation of Water Indices for Surface Water Extraction in a Landsat 8 Scene of Nepal. *Sensors*, *18*(8), 2580.

Akinola, A. I., Wynn-Thompson, T., Olgun, C. G., Mostaghimi, S., & Eick, M. J. (2019). Fluvial Erosion Rate of Cohesive Streambanks Is Directly Related to the Difference in Soil and Water Temperatures. *Journal of Environmental Quality*, *48*(6), 1741–1748. https://doi.org/https://doi.org/10.2134/jeq2018.10.0385

Allen, G. H., & Pavelsky, T. M. (2018). Global extent of rivers and streams. *Science*, *361*(6402), 585–588. https://doi.org/10.1126/science.aat0636

Altenau, E. H., Pavelsky, T. M., Durand, M. T., Yang, X., Frasson, R. P. d. M., & Bendezu, L. (2021). The Surface Water and Ocean Topography (SWOT) Mission River Database (SWORD): A Global River Network for Satellite Data Products. *Water Resources Research*, *57*(7), e2021WR030054. https://doi.org/https://doi.org/10.1029/2021WR030054

Anderson, R. J., Bledsoe, B. P., & Hession, W. C. (2004). WIDTH OF STREAMS AND RIVERS IN RESPONSE TO VEGETATION, BANK MATERIAL, AND OTHER FACTORS. *JAWRA Journal of the American Water Resources Association*, *40*(5), 1159–1172. https://doi.org/https://doi.org/10.1111/j.1752-1688.2004.tb01576.x

Boothroyd, R. J., Williams, R. D., Hoey, T. B., Brierley, G. J., Tolentino, P. L. M., Guardian, E. L., Reyes, J. C. M. O., Sabillo, C. J., Quick, L., Perez, J. E. G., & David, C. P. C. (2025). Big data show idiosyncratic patterns and rates of geomorphic river mobility. *Nature Communications*, *16*(1), 3263. https://doi.org/10.1038/s41467-025-58427-9

Braudrick, C. A., Dietrich, W. E., Leverich, G. T., & Sklar, L. S. (2009). Experimental evidence for the conditions necessary to sustain meandering in coarse-bedded rivers. *Proceedings of the National Academy of Sciences*, *106*(40), 16936–16941. https://doi.org/10.1073/pnas.0909417106

Bywater-Reyes, S., Diehl, R. M., & Wilcox, A. C. (2018). The influence of a vegetated bar on channel-bend flow dynamics. *Earth Surf. Dynam.*, *6*(2), 487–503. https://doi.org/10.5194/esurf-6-487-2018

Chen, F., Chen, X., Van de Voorde, T., Roberts, D., Jiang, H., & Xu, W. (2020). Open water detection in urban environments using high spatial resolution remote sensing imagery. *Remote Sensing of Environment*, *242*, 111706. https://doi.org/https://doi.org/10.1016/j.rse.2020.111706

Chin, A. (2006). Urban transformation of river landscapes in a global context. *Geomorphology*, *79*(3), 460–487. https://doi.org/https://doi.org/10.1016/j.geomorph.2006.06.033

Cohen, S., Syvitski, J., Ashley, T., Lammers, R., Fekete, B., & Li, H.-Y. (2022). Spatial Trends and Drivers of Bedload and Suspended Sediment Fluxes in Global Rivers. *Water Resources Research*, *58*(6), e2021WR031583. https://doi.org/https://doi.org/10.1029/2021WR031583

Constantine, J. A., Dunne, T., Ahmed, J., Legleiter, C., & Lazarus, E. D. (2014). Sediment supply as a driver of river meandering and floodplain evolution in the Amazon Basin. *Nature Geoscience*, *7*(12), 899–903. https://doi.org/10.1038/ngeo2282

https://doi.org/10.5194/egusphere-2026-4621
Preprint. Discussion started: 12 August 2026

Darby, S. E., Alabyan, A. M., & Van de Wiel, M. J. (2002). Numerical simulation of bank erosion and channel migration in meandering rivers. *Water Resources Research*, *38*(9), 2–1–2–21. https://doi.org/https://doi.org/10.1029/2001WR000602

Darby, S. E., Rinaldi, M., & Dapporto, S. (2007). Coupled simulations of fluvial erosion and mass wasting for cohesive river banks. *Journal of Geophysical Research: Earth Surface*, *112*(F3). https://doi.org/https://doi.org/10.1029/2006JF000722

Deoli, V., Kumar, D., & Kuriqi, A. (2022). Detection of Water Spread Area Changes in Eutrophic Lake Using Landsat Data. *Sensors*, *22*(18), 6827. https://doi.org/10.3390/s22186827

Dietrich, Smith, J. D., & Dunne, T. (1979). Flow and Sediment Transport in a Sand Bedded Meander. *The Journal of Geology*, *87*(3), 305–315.

Du, Y., Zhang, Y., Ling, F., Wang, Q., Li, W., & Li, X. (2016). Water Bodies' Mapping from Sentinel-2 Imagery with Modified Normalized Difference Water Index at 10-m Spatial Resolution Produced by Sharpening the SWIR Band. *Remote Sensing*, *8*(4), 354. https://doi.org/10.3390/rs8040354

Eke, E., Parker, G., & Shimizu, Y. (2014). Numerical modeling of erosional and depositional bank processes in migrating river bends with self-formed width: Morphodynamics of bar push and bank pull. *Journal of Geophysical Research: Earth Surface*, *119*(7), 1455–1483. https://doi.org/https://doi.org/10.1002/2013JF003020

Feng, D., Gleason, C. J., Yang, X., Allen, G. H., & Pavelsky, T. M. (2022). How Have Global River Widths Changed Over Time? *Water Resources Research*, *58*(8), e2021WR031712. https://doi.org/https://doi.org/10.1029/2021WR031712

Finotello, A., Ielpi, A., Lapôtre, M. G. A., Lazarus, E. D., Ghinassi, M., Carniello, L., Favaro, S., Tognin, D., & D'Alpaos, A. (2024). Vegetation enhances curvature-driven dynamics in meandering rivers. *Nature Communications*, *15*(1), 1968. https://doi.org/10.1038/s41467-024-46292-x

Francalanci, S., Lanzoni, S., Solari, L., & Papanicolaou, A. N. (2020). Equilibrium Cross Section of River Channels With Cohesive Erodible Banks. *Journal of Geophysical Research: Earth Surface*, *125*(1), e2019JF005286. https://doi.org/https://doi.org/10.1029/2019JF005286

Galia, T., Poledniková, Z., & Škarpich, V. (2024). Impact of large wood on sediment (dis)connectivity in a meandering river. *Geomorphology*, *453*, 109153. https://doi.org/https://doi.org/10.1016/j.geomorph.2024.109153

Gautam, V. K., Gaurav, P. K., Murugan, P., & Annadurai, M. (2015). Assessment of Surface Water Dynamicsin Bangalore Using WRI, NDWI, MNDWI, Supervised Classification and K-T Transformation. *Aquatic Procedia*, *4*, 739–746. https://doi.org/https://doi.org/10.1016/j.aqpro.2015.02.095

Gualtieri, C., Abdi, R., Ianniruberto, M., Filizola, N., & Endreny, T. A. (2020). A 3D analysis of spatial habitat metrics about the confluence of Negro and Solimões rivers, Brazil. *Ecohydrology*, *13*(1). https://doi.org/10.1002/eco.2166

Herndon, K., Muench, R., Cherrington, E., & Griffin, R. (2020). An Assessment of Surface Water Detection Methods for Water Resource Management in the Nigerien Sahel. *Sensors*, *20*(2), 431. https://doi.org/10.3390/s20020431

Hersbach, H., Bell, B., Berrisford, P., Biavati, G., Horányi, A., Muñoz Sabater, J., Nicolas, J., Peubey, C., Radu, R., Rozum, I., Schepers, D., Simmons, A., S., C., , Dee, D., & Thépaut, J.-N. (2024). *ERA5 hourly data on pressure levels from 1940 to present* (

Hickin, E. J., & Nanson, G. C. (1975). The Character of Channel Migration on the Beatton River, Northeast British Columbia, Canada. *GSA Bulletin*, *86*(4), 487–494. https://doi.org/10.1130/0016-7606(1975)86<487:Tcocmo>2.0.Co;2

Ielpi, A., & Lapôtre, M. G. A. (2020). A tenfold slowdown in river meander migration driven by plant life. *Nature Geoscience*, *13*(1), 82–86. https://doi.org/10.1038/s41561-019-0491-7

Ikeda, S., Parker, G., & Sawai, K. (1981). Bend theory of river meanders. Part 1. Linear development. *Journal of Fluid Mechanics*, *112*, 363–377. https://doi.org/10.1017/S0022112081000451

Inoue, T., Hiramatsu, Y., Johnson, J. P. L., Dempo, J., & Mishra, J. (2025). Ratio of River Channel Bar to Bank Height Sets Bank Erosion Rate. *Journal of Geophysical Research: Earth Surface*, *130*(1), e2024JF007965. https://doi.org/https://doi.org/10.1029/2024JF007965

Jarchow, C. J., Nagler, P. . (2019). *Enhanced Vegetation Index (EVI) parameter data products from Landsat 5, Landsat 8 MODIS and the Visible Infrared Imaging Radiometer Suite (VIIRS)* (https://doi.org/https://doi.org/10.5066/P9UMMJ9S

Jepsen, R., Roberts, J., & Lick, W. (1997). Effects of bulk density on sediment erosion rates. *Water, Air, and Soil Pollution*, *99*(1), 21–31. https://doi.org/10.1007/BF02406841

Kottek, M., Grieser, J., Beck, C., Rudolf, B., & Rubel, F. (2006). World Map of the Köppen-Geiger Climate Classification Updated. *Meteorologische Zeitschrift*, *15*, 259–263. https://doi.org/10.1127/0941-2948/2006/0130

Krzeminska, D., Kerkhof, T., Skaalsveen, K., & Stolte, J. (2019). Effect of riparian vegetation on stream bank stability in small agricultural catchments. *CATENA*, *172*, 87–96. https://doi.org/https://doi.org/10.1016/j.catena.2018.08.014

Langendoen, E., Wells, R., Thomas, R., Simon, A., & Bingner, R. (2009). Modeling the Evolution of Incised Streams. III: Model Application. *Journal of Hydraulic Engineering-asce - J HYDRAUL ENG-ASCE*, *135*. https://doi.org/10.1061/(ASCE)HY.1943-7900.0000029

Langhorst, T., & Pavelsky, T. (2023). Global Observations of Riverbank Erosion and Accretion From Landsat Imagery. *Journal of Geophysical Research: Earth Surface*, *128*(2), e2022JF006774. https://doi.org/https://doi.org/10.1029/2022JF006774

Leenman, A. S., Slater, L. J., Dadson, S. J., Wortmann, M., & Boothroyd, R. (2023). Quantifying the Geomorphic Effect of Floods Using Satellite Observations of River Mobility. *Geophysical Research Letters*, *50*(16), e2023GL103875. https://doi.org/https://doi.org/10.1029/2023GL103875

Linke, S., Lehner, B., Ouellet Dallaire, C., Ariwi, J., Grill, G., Anand, M., Beames, P., Burchard-Levine, V., Maxwell, S., Moidu, H., Tan, F., & Thieme, M. (2019). Global hydro-environmental sub-basin and river reach characteristics at high spatial resolution. *Scientific Data*, *6*(1), 283. https://doi.org/10.1038/s41597-019-0300-6

Lopez Dubon, S., & Lanzoni, S. (2019). Meandering Evolution and Width Variations: A Physics-Statistics-Based Modeling Approach. *Water Resources Research*, *55*(1), 76–94. https://doi.org/https://doi.org/10.1029/2018WR023639

Luize, B. G., Magalhães, J. L. L., Queiroz, H., Lopes, M. A., Venticinque, E. M., Leão De Moraes Novo, E. M., & Silva, T. S. F. (2018). The tree species pool of Amazonian wetland forests: Which species can assemble in periodically waterlogged habitats? *PLOS ONE*, *13*(5), e0198130. https://doi.org/10.1371/journal.pone.0198130

Mahmoud, B. M. M., Trudel, M., Biron, P. M., Sklar, L. S., & Lacey, J. (2026). River Meander Development by Bar-Push and Bank-Pull During Cyclic Hydrographs in a Field-Scale Experimental Channel. *Water Resources Research*, *62*(5), e2025WR043155. https://doi.org/https://doi.org/10.1029/2025WR043155

Martin, H., Edmonds, D., & Lewis, Q. (2024). Four Years of Meander-Bend Evolution Captured by Drone-Based Lidar Reveals Lack of Width Maintenance on the White River, Indiana, USA. *Journal of Geophysical Research: Earth Surface*, *129*. https://doi.org/10.1029/2023JF007574

Mason, J., & Mohrig, D. (2018). Using Time-Lapse Lidar to Quantify River Bend Evolution on the Meandering Coastal Trinity River, Texas, USA. *Journal of Geophysical Research: Earth Surface*, *123*(5), 1133–1144. https://doi.org/https://doi.org/10.1029/2017JF004492

McNabb, D. H., Startsev, A. D., & Nguyen, H. (2001). Soil Wetness and Traffic Level Effects on Bulk Density and Air-Filled Porosity of Compacted Boreal Forest Soils. *Soil Science Society of America Journal*, *65*(4), 1238–1247. https://doi.org/https://doi.org/10.2136/sssaj2001.6541238x

Nagabhushanaiah, H. S. (1967). MEANDERING OF RIVERS. *International Association of Scientific Hydrology. Bulletin*, *12*(1), 28–43. https://doi.org/10.1080/02626666709493509

Nagel, G., Darby, S., & Leyland, J. (2025). *Surface Water Transitions 1984-2022: A Global Dataset at Annual Resolution*.

Nagel, G. W., de Moraes Novo, E. M. L., Martins, V. S., Campos-Silva, J. V., Barbosa, C. C. F., & Bonnet, M. P. (2022). Impacts of meander migration on the Amazon riverine communities using Landsat time series and cloud computing. *Science of the Total Environment*, *806*, 150449. https://doi.org/https://doi.org/10.1016/j.scitotenv.2021.150449

Parker, G., Shimizu, Y., Wilkerson, G. V., Eke, E. C., Abad, J. D., Lauer, J. W., Paola, C., Dietrich, W. E., & Voller, V. R. (2011). A new framework for modeling the migration of meandering rivers. *Earth Surface Processes and Landforms*, *36*(1), 70–86. https://doi.org/https://doi.org/10.1002/esp.2113

Phillips, C. B., Masteller, C. C., Blaylock, J., Van Iwaarden, F., & Johnson, J. P. L. (2024). Variability in River Width Reveals Climatic Influence on Channel Geometry. *Geophysical Research Letters*, *51*(23), e2024GL111789. https://doi.org/https://doi.org/10.1029/2024GL111789

Poggio, L., de Sousa, L. M., Batjes, N. H., Heuvelink, G. B. M., Kempen, B., Ribeiro, E., & Rossiter, D. (2021). SoilGrids 2.0: producing soil information for the globe with quantified spatial uncertainty. *SOIL*, *7*(1), 217–240. https://doi.org/10.5194/soil-7-217-2021

Ratner, B. (2009). The correlation coefficient: Its values range between +1/−1, or do they? *Journal of Targeting, Measurement and Analysis for Marketing*, *17*(2), 139–142. https://doi.org/10.1057/jt.2009.5

Rokni, K., Ahmad, A., Selamat, A., & Hazini, S. (2014). Water Feature Extraction and Change Detection Using Multitemporal Landsat Imagery. *Remote Sensing*, *6*(5), 4173–4189. https://doi.org/10.3390/rs6054173

https://doi.org/10.5194/egusphere-2026-4621
Preprint. Discussion started: 12 August 2026

Sabo, J. L., Sponseller, R., Dixon, M., Gade, K., Harms, T., Heffernan, J., Jani, A., Katz, G., Soykan, C., Watts, J., & Welter, J. (2005). Riparian Zones Increase Regional Species Richness by Harboring Different, Not More, Species. *Ecology*, *86*(1), 56–62. https://doi.org/https://doi.org/10.1890/04-0668

Sarp, G., & Ozcelik, M. (2017). Water body extraction and change detection using time series: A case study of Lake Burdur, Turkey. *Journal of Taibah University for Science*, *11*(3), 381–391. https://doi.org/10.1016/j.jtusci.2016.04.005

Schumm, S. A., & Khan, H. R. (1971). Experimental Study of Channel Patterns. *Nature*, *233*(5319), 407–409. https://doi.org/10.1038/233407a0

Schwendel, A. C., Nicholas, A. P., Aalto, R. E., Sambrook Smith, G. H., & Buckley, S. J. (2015). Interaction between meander dynamics and floodplain heterogeneity in a large tropical sand-bed river: the Rio Beni, Bolivian Amazon. *Earth Surface Processes and Landforms*, *40*, 2026 – 2040.

Simon, A., & Collison, A. J. C. (2002). Quantifying the mechanical and hydrologic effects of riparian vegetation on streambank stability. *Earth Surface Processes and Landforms*, *27*(5), 527–546. https://doi.org/https://doi.org/10.1002/esp.325

Sylvester, Z., Durkin, P., & Covault, J. A. (2019). High curvatures drive river meandering. *Geology*, *47*(3), 263–266. https://doi.org/10.1130/g45608.1

Van De Lageweg, W. I., Van Dijk, W. M., Baar, A. W., Rutten, J., & Kleinhans, M. G. (2014). Bank pull or bar push: What drives scroll-bar formation in meandering rivers? *Geology*, *42*(4), 319–322. https://doi.org/10.1130/g35192.1

van Dijk, W. M., Teske, R., van de Lageweg, W. I., & Kleinhans, M. G. (2013). Effects of vegetation distribution on experimental river channel dynamics. *Water Resources Research*, *49*(11), 7558–7574. https://doi.org/https://doi.org/10.1002/2013WR013574

van Dijk, W. M., van de Lageweg, W. I., & Kleinhans, M. G. (2012). Experimental meandering river with chute cutoffs. *Journal of Geophysical Research: Earth Surface*, *117*(F3). https://doi.org/https://doi.org/10.1029/2011JF002314

Worden, J., & de Beurs, K. M. (2020). Surface water detection in the Caucasus. *International Journal of Applied Earth Observation and Geoinformation*, *91*, 102159. https://doi.org/https://doi.org/10.1016/j.jag.2020.102159

Xu, H. (2006). Modification of normalised difference water index (NDWI) to enhance open water features in remotely sensed imagery. *International Journal of Remote Sensing*, *27*(14), 3025–3033. https://doi.org/10.1080/01431160600589179

Zhu, L., Chen, D., Hassan, M. A., & Venditti, J. G. (2022). The Influence of Riparian Vegetation on the Sinuosity and Lateral Stability of Meandering Channels. *Geophysical Research Letters*, *49*(2), e2021GL096346. https://doi.org/https://doi.org/10.1029/2021GL096346

Zinger, J. A., Rhoads, B. L., Best, J. L., & Johnson, K. K. (2013). Flow structure and channel morphodynamics of meander bend chute cutoffs: A case study of the Wabash River, USA. *Journal of Geophysical Research: Earth Surface*, *118*(4), 2468–2487. https://doi.org/10.1002/jgrf.20155